A HIGH SPEED BACK PROPAGATION NEURAL NETWORK FOR MULTISTAGE MR BRAIN TUMOR IMAGE SEGMENTATION

*D. Jude Hemanth, C. Kezi Selva Vijila, J. Anitha**

Abstract: Artificial neural networks (ANN) are one of the highly preferred artificial intelligence techniques for brain image segmentation. The commonly used ANN is the supervised ANN, namely Back Propagation Neural Network (BPN). Even though BPNs guarantee high efficiency, they are computationally non-feasible due to the huge convergence time period. In this work, the aspect of computational complexity is tackled using the proposed high speed BPN algorithm (HSBPN). In this modified approach, the weight vectors are calculated without any training methodology. Magnetic resonance (MR) brain tumor images of three stages, namely severe, moderate and mild, are used in this work. An extensive feature set is extracted from these images and used as input for the neural network. A comparative analysis is performed between the conventional BPN and the HSBPN in terms of convergence time period and segmentation efficiency. Experimental results show the superior nature of HSBPN in terms of the performance measures.

Key words: *Back propagation, neural network, MR brain image, high speed BPN, convergence time period*

Received: August 3, 2009
Revised and accepted: January 27, 2011

1. Introduction

Accurate and robust brain tissue segmentation from Magnetic Resonance (MR) images is a very important issue in many applications of medical image analysis. One significant application is the quantitative estimation of the growth process of brain tumors [1]. The abnormal tumor portions are often distinguished from the normal tissues by analyzing the texture and the intensity of the abnormal region which is usually different from healthy tissues. The segmentation of tumor

*D. Jude Hemanth, C. Kezi Selva Vijila, J. Anitha
Department of ECE, Karunya University, Coimbatore, India, E-mail:
jude_hemanth@rediffmail.com, vijila2000@yahoo.com, rajivee1@rediffmail.com

tissues is a challenging task because there are a large number of tumor types which greatly differ in size, shape, tissue composition and tissue homogeneity [2]. The segmentation of tumor portion is performed manually with the help of the special marker pencil. These markers are used to trace the boundaries of the abnormal portion. In some cases, the boundary of the tumor tissues is not well defined, which is very difficult for the radiology experts to delineate. Manual tracing of tumor by an expert is not only time-consuming but also exhausting for experts, which can lead to human errors [3]. Therefore, an automatic segmentation technique with high accuracy and excellent robustness is necessary for brain tumor segmentation in the medical field.

Numerous studies of brain tumor segmentation have been carried out and are reported in the literature. The methods based on elastic registration using elastic matching techniques or deformable models [4] have proven to be reliable and efficient for small and local shape changes. The methods based on statistical models, such as Gaussian intensity models [5], explicit models [6], Markov random field models [7], work well in the case of brain tissue segmentation. Level set methods are also used for brain tumor segmentation [8] with some success. In spite of the power of these kinds of approaches, some of them need manual tracing [9] for the initialization or a semi-supervised system [10] with some manual learning.

Another group of research highly depends on the artificial intelligence techniques for brain tumor segmentation. Among the artificial intelligence techniques, artificial neural networks are widely employed for brain tumor segmentation. Zumray et al. [11] elaborates the inferior results of multilayer perceptron for the biomedical image classification problem. The Self Organizing Feature Map (SOFM) ANN based algorithms [12] show excellent results in the segmentation of brain tumor images. Other studies based on learning vector quantization (LVQ) [13] ANN show the potential of these architectures in the case of supervised classification. Hopfield neural networks (HNN) [14] also prove to be efficient for unsupervised pattern classification of medical images, particularly in the detection of abnormal tissues. Back propagation neural networks [15] are also used for image segmentation applications and these neural networks are considered in this study for brain tumor segmentation. Besides being robust, they require large training dataset to achieve high accuracy. This increases the dimensionality problem which accounts for the long convergence time period, which makes the system practically non-feasible. An improved version of back propagation algorithm is used for breast cancer detection [16]. Changhua [17] implemented the multilayer feed forward network with a modified training algorithm. A different version of BPN is employed for pattern recognition [18].

In this work, a modified BPN namely high speed back propagation neural network (HSBPN) is proposed for multistage brain tumor image segmentation. The suitability of the proposed method for segmenting the tumor with less convergence time period is explored in this paper. The technique is experimented on brain tumor images of three stages, namely severe, mild and moderate, to show that the proposed methodology works well for varying tumor size and shapes. A quantitative and qualitative comparison is done with the conventional BPN to show the superior nature of HSBPN in terms of the performance measures. Experimental results show promising results for the proposed network.

2. Proposed Methodology

The proposed methodology of the automated image segmentation system is shown in Fig. 1.

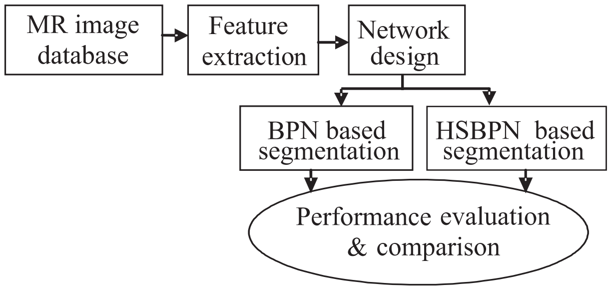

Fig. 1 *Proposed methodology.*

The framework of the image segmentation system is divided into following categories, viz: short description on the input dataset, methods of feature extraction, method of BPN architecture selection, image segmentation using BPN and HSBPN, and finally performance estimation and comparison.

3. Input Dataset and Feature Extraction

3.1 MR image database

The MR images used in this work are obtained from the `http://www.bic.mni.mcgill.ca/brainweb` website in the Montreal Neurological Institute, McGill University, McConnell Brain Imaging Centre (McBIC) [19]. The database is the result of a research work developed at McBIC and contains quantitative 3D investigation of brain structure and function. The brain phantom and simulated MR images have been made publicly available and can be used to test algorithms. Brain tumor images of three different stages and their ground truth are available and were primarily used in this work. All the images are gray intensity images with the dimension of 256×256.

3.2 Feature extraction

The purpose of feature extraction is to reduce the original data set by measuring certain properties, or features that distinguish one input pattern from another pattern. The extracted feature should provide the characteristics of the input type to the classifier by considering the description of the relevant properties of the image into a feature space. Five textural features based on Gray level Co-occurrence Matrix (GLCM), namely energy, entropy, correlation, variance and inverse difference moment, are used for training the BPN in this work. Haarlick [20] suggested the use of gray level co-occurrence matrices (GLCM) which have become one of the most well-known and widely used texture features. GLCM $\{P_{(d,\theta)}\ (i,j)\}$ represents the probability of occurrence of a pair of gray-levels (i,j) separated by a given distance $d$at angle θ. The commonly used pixel distance is one and the pixel to the immediate right of the pixel of interest is considered. The commonly used angles are 0°, 45°, 90° and 135°. A detailed algorithm of calculation of GLCM $\{P_{(d,\theta)}\ (i,j)\}$ has been given in [21]. In this work, a GLCM of size P (256, 256) is generated. The features, such as energy, entropy, correlation, variance and inverse difference moment, are calculated using the formulae given below. The following notations are used in the formulae.

$p(i,j)$ = GLCM of size 256*256.

$p(x)$ = Horizontal summation of the vector elements of $p(i, j)$; size = (256*1)

$p(y)$ = Vertical summation of the vector elements of $p(i, j)$; size = (1*256)

Inverse difference moment:

$$S_I = \sum_i \sum_j \frac{1}{1+(i-j)^2} p(i,j)\,; i = 1, 2 \ldots 256; j = 1, 2 \ldots 256 \tag{1}$$

Correlation:

$$S_O = \frac{\sum_i \sum_j (ij)\, p(i,j) - \mu_x \mu_y}{\sigma_x \sigma_y} \tag{2}$$

where $\mu_x, \mu_y, \sigma_x, \sigma_y$ are the means and standard deviations of p_x and p_y.

Variance:

$$S_V = \sum_i \sum_j (i-\mu)^2 p(i,j) \tag{3}$$

where μ = mean of GLCM.

Entropy:

$$S_F = -\sum p(i,j) \log \{p(i,j)\} \tag{4}$$

Energy:

$$S_N = \sum [p(i,j)]^2 \tag{5}$$

The features used in this paper are selected based on the previous works [20, 22]. These features work well especially for MRI brain tumor images. Prior to training, the selection of architecture plays a vital role in determining the segmentation efficiency.

4. Network Design

In this work, a three layer network is developed. An input vector and the corresponding desired output are considered first. The input is propagated forward through the network to compute the output vector. The output vector is compared with the desired output and the training errors are determined. The errors are then propagated back through the network from the output to input layer. The process is repeated until the errors are minimized. The input layer of network consists of 5 neurons corresponding to 5 input features. The output layer consists of 4 neurons corresponding to 4 predefined categories, such as the white matter, gray matter, Cerebro Spinal Fluid (CSF) and the abnormal tumor region. When designing a neural network, one crucial and difficult step is determining the number of neurons in the hidden layers. If there are too few neurons in the hidden layer, the network may not contain sufficient degrees of freedom to form a representation. If too many neurons are defined, the network might become over trained [23]. Therefore, an optimum design for the number of neurons in the hidden layer is required. In this research, one hidden layer is used with a number of different neurons to determine the suitable network. Tab. I shows the training error of network for five cases.

Class	Training data (pixels/image)	Error (%)				
		(a) k = 4	(b) k = 8	(c) k = 12	(d) k = 16	(e) k = 20
White matter	40	8	9	2	7	9
Gray matter	40	2	1	0	1	4
CSF	40	12	9	2	8	12
Tumor	20	2	1	0	0	3
Average		6	5	1	4	7

Tab. I *Four networks with different neurons 'k' in hidden layer.*

Initially, pixels from the four classes are used to train the BPN with 4 neurons in the hidden layer. The training data consists of 40 pixels from each of the normal tissue type and 20 pixels for the abnormal tissue type. These values are selected randomly and since the abnormal portion of the image is very small, the training data consists of less number of abnormal tissue pixels than the normal tissue pixels. The network is trained with few pixels (from each image) from each class, and the training error (Mean square error) is observed with the error tolerance value of 0.01. This procedure is repeated with different neurons (4 to 20) in the hidden layer of the BPN. The average error value for all the classes with different neurons in the hidden layer is calculated. The error values for BPN with 4, 8, 12, 16, 20 hidden neurons are shown in Tab. I. As seen in Tab. I, the error decreases and reaches a minimum value at $k = 12$ and then it increases. A network with 12 neurons in hidden layer has the minimum error, so it is the best case for designing network in this case. Thus architecture of 5-12-4 for the BPN is used in this work.

5. Artificial neural Network Based Segmentation

Back propagation network is the primarily used supervised artificial neural network. In this work, a modification of the existing BPN is proposed for brain tumor image segmentation.

5.1 Conventional back propagation neural network

Back propagation neural network belongs to the supervised feed forward neural network category. It is framed by generalizing the Widrow-Hoff learning rule to multiple layer network and non-linear differentiable transfer function. Input vectors and the corresponding target vectors are used to train the network until it classify input vectors in an appropriate way, as defined in this study.

Architecture. As per the network design, the architecture of the BPN is shown in Fig. 2.

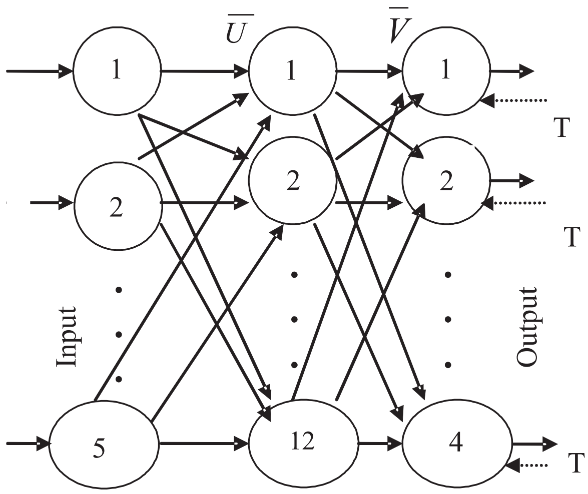

Fig. 2 *Topology of BPN.*

The input layer and the hidden layer neurons are interconnected by the set of weight vectors $\overline{U}$and the hidden layer and the output layer neurons are interconnected by the weight matrix $\overline{V}$. In addition to the input vector X and output vector Y, the target vector T is given to the output layer neurons. Since BPN operates in the supervised mode, the target vector is mandatory. During the training process, the difference between the output vector and the target vector is calculated and the weight values are updated based on the difference value.

Training algorithm. The training algorithm of BPN involves three stages: the feed forward of the input training pattern, the back propagation of the associated error and the adjustment of the weights. The training algorithm is summarized as follows:

Step 1: Initialize the weights u_{ij} and v_{jk}.
Step 2: For each training pair, do steps 3-9.

Feed forward

Step 3: Each input unit (x_i) receives the input signal and broadcasts the signals to the hidden layer neurons (z_j), where $i = 1, 2......5$ and $j = 1, 2....12$.

Step 4: Each hidden unit sums its weighted input signals

$$z\_in_j = \sum x_i \cdot u_{ij} \tag{6}$$

and applies it to the activation function to compute its output signal,

$$z_j = f\left(z\_in_j\right). \tag{7}$$

The activation function used in this work is sigmoid function.

This output signal is fed to the output layer neurons (y_k) where $k = 1, 2...4$.

Step 5: Each output unit sums its weighted input signals

$$y\_in_k = \sum z_j \cdot v_{jk} \tag{8}$$

and applies its activation function (sigmoidal function) to compute its output signal

$$y_k = f\left(y\_in_k\right). \tag{9}$$

Back propagation of error

Step 6: Each output unit receives a target pattern (t_k) and compute its error information term

$$\delta_k = (t_k - y_k) \cdot f'\left(y\_in_k\right) \tag{10}$$

and calculates the weight correction term

$$\Delta v_{jk} = \alpha \cdot \delta_k \cdot z_j, \tag{11}$$

where α = learning rate.

Step 7: Each hidden unit computes its error information term

$$\delta_j = \sum \delta_k v_{jk} \cdot f'\left(z\_in_j\right) \tag{12}$$

and calculates the weight correction term

$$\Delta u_{ij} = \alpha \cdot \delta_j \cdot x_i. \tag{13}$$

Update weights

Step 8: Each output unit updates its weights by

$$v_{jk}\,(new) = v_{jk}\,(old) + \Delta v_{jk}. \tag{14}$$

Each hidden unit updates its weights by

$$u_{ij}\,(new) = u_{ij}\,(old) + \Delta u_{ij}. \tag{15}$$

Step 9: The training stops when the weight correction term in Eqn. (14) and Eqn. (15) are equal to zero (or) a predefined minimum value which indirectly indicates $(t_k - y_k)$ equal to zero (or) a predefined minimum value.

This methodology of training is computationally tedious, which accounts for the slow convergence. Since the hidden layer is not directly connected with the target vector, the mathematical operations for weight adjustment in the hidden layer are significantly high, which also adds to the complexity. These drawbacks are tackled in the proposed modified BPN, namely high speed back propagation neural network (HSBPN) which is explained in the next section.

5.2 High speed back propagation neural network

The high speed back propagation neural network is framed by performing two modifications in the architecture and the training algorithm of the conventional BPN. These two modifications enhance the performance of the existing Back propagation neural network in terms of accuracy and convergence time period.

In terms of architecture, the target vectors are supplied to the hidden layer in addition to the output layer neurons in the HSBPN. This may result in dimension mismatch problem between the input vector and the target vector but it can be solved by representing the same target vector in a different manner. Since four classes are used in this work, the target vector given to the output layer is represented by 4 bits whereas the same target vector supplied to the hidden layer is represented by 12 bits. Thus, the target vector is supplied to both the hidden layer and the output layer without any complications.

In terms of training algorithm, there is no necessity for the weight adjustment criterion in the HSBPN. Since the target vector is given to both the hidden and the output layers, the multilayer HSBPN can be considered as two single layer networks with independent weight calculation procedure for both the layers. The error is calculated for each layer and the weights are adjusted accordingly, which avoids the complex mathematical calculations involved in training the weights between the input layer and the hidden layer in the conventional BPN. Since this network is devoid of training, the convergence time period is very less when compared with the conventional BPN.

HSBPN Architecture. The architecture of the proposed HSBPN is shown in Fig. 3.

In the above figure, dashed lines are used to represent the target vector which is supplied to the neurons in the hidden layer and the output layer. Hence, this multilayer network can be divided into two supervised single layer networks with the same target vector: one with the input layer and the hidden layer with x_i as inputs and the other with the hidden layer and the output layer with z_j as inputs. The topology of the HSBPN is 5-12-4.

Training algorithm. The main objective of the training methodology of the conventional BPN is to calculate the weight matrices by minimizing the error value. In this modified algorithm, the weight matrices are calculated without any training methodology. The steps of the conventional training algorithm are followed but in reverse direction. The detailed steps of the HSBPN algorithm are given below.

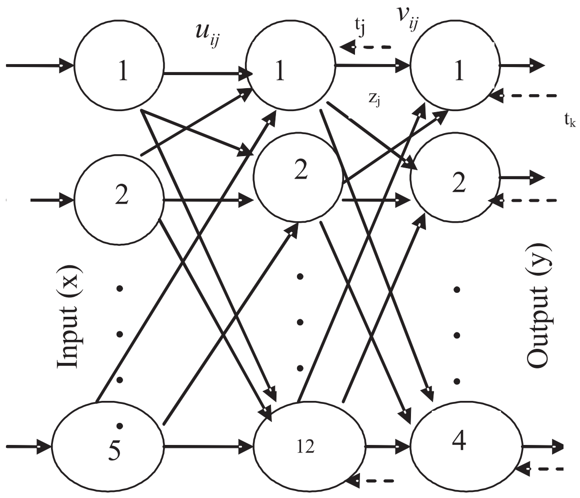

Fig. 3 *Topology of HSBPN.*

Step 1: The stabilized weight values are obtained when the error value (target-output) is equal to zero (or) a predefined minimum value. The error value used for convergence in this work is 0.01. The following procedure uses this concept for weight matrices calculation.

Step2: Four training pairs are formed by averaging the feature values of the training pixels of each class. For each training pair, do steps 3-8.

Calculation of weight matrix between input layer and hidden layer

Step 3: Since $(t_j - z_j) = 0.01$ for convergence, the output of the hidden layer neurons is set equal to the target values

$$z_j = t_j - 0.01, \tag{16}$$

where t_j is the target supplied to the hidden layer.

Step 4: Once the output value is calculated, Eqn. (7) is used to calculate the sum of the weighted input signals (z_in_j). Since the sigmoid activation function is used, the following equation yields the value forz_in_j.

$$z\_in_j = \quad \ln\left[\frac{z_j}{|1 - z_j|}\right] \tag{17}$$

Step 5: Based on the values ofz_in_j, the weight matrix u_{ij} is calculated using Eqn. (6). The matrix equation is solved using Math toolbox in MATLAB.

Calculation of weight matrix between hidden layer and output layer

Step 6: Using the condition in step 3, the output value is set equal to the target value

$$y_k = t_k - 0.01 \tag{18}$$

Step 7: The same procedure in step 4 is used to calculate the value for y_in_k

$$y\_in_k = \ln\left[\frac{y_k}{|1-y_k|}\right] \tag{19}$$

Step 8: Since the values of z_j and y_in_k are known, the weight matrix v_{jk} is calculated using Eqn. (8). The matrix equation is solved using Math toolbox in MATLAB.

Thus, four weight matrices are calculated for the four training pairs corresponding to four classes. These weight calculations are devoid of training, which reduces the convergence time period. The weight values are calculated based on the convergence condition and, hence, these represent the stabilized weight matrix. Since error value of zero is not always possible in practical applications, error values such as 0.01, 0.001 can be used, which does not have much impact on Eqn. (16) and Eqn. (18). The dimension mismatch problem in supplying the target vector to the hidden layer is solved by different representation of the target vector.

The testing of the unknown pixels is performed by considering the network as a multilayer supervised neural network with all the four weight matrices individually. In each case, the difference between the output and target is calculated and the pixel is allotted to the class for which the difference is minimum. The testing time period is slightly higher than the conventional BPN but the overall convergence time period of HSBPN is very much shorter than the conventional BPN.

6. Implementation

The proposed algorithm is experimented on MR brain tumor images of different stages, such as mild, moderate and severe. The training and the testing dataset used in this work is shown in Tab. II.

Class	Training data (pixels/ image)	Testing data (pixels/image)
White matter	40	65536 (Full image)
Grey matter	40	
CSF	40	
Tumor	20	

Tab. II *Data set for image segmentation.*

In this work, 140 training points are chosen according to their location in the phantom images to generate the correspondence between the pixels and the corresponding class. Five textural features are extracted from these training points. The average of the feature values for each class are calculated and supplied as training inputs. The network is tested with the whole image.

The GLCM matrix (p(i, j)) is obtained by averaging the individual GLCM matrix at four primary angles, such as 0^o, 45^o, 90^o and 135^o. The mode of training used in HSBPN is batch mode training in which all the training feature values are applied sequentially to the input layer. The error tolerance value used for training the conventional BPN and HSBPN is 0.01. The learning rate used for training conventional BPN is 0.8. The target values used for training the output layer of HSBPN are [1 2 3 4]. The target values used for training the hidden layer of HSBPN are [1 1 1 2 2 2 3 3 3 4 4 4]. Since the hidden layer consists of 12 neurons, each class is represented by 12 bits with the class number denoted by the first 3 bits. The activation function used for training BPN and HSBPN is sigmoidal activation function.

The experiments are carried out on an IBM PC Pentium with processor speed 700 MHz and 256 MB RAM. The software used for the implementation is MATLAB (version 7.0) [24], developed by Math works Laboratory.

7. Results and Discussions

The abovemodified BPN is employed to segment MR images into four groups. Among the four groups, the region of interest is the abnormal tumor region. This technique is experimented on brain tumor images of three stages, such as mild, moderate and severe. The segmentation is also performed with the conventional BPN to show the superior nature of HSBPN. The performance measures used in this work are segmentation efficiency and convergence time period. Fig. 4 shows the qualitative results of segmentation of the severe brain tumor image.

The qualitative comparison of the phantom images and the segmented images in Fig. 4 shows the superior nature of the proposed method in segmenting the inner tissues, such as tumor region. The segmentation is not so clear in the other tissues since there is no clear classification of external tissues. The skull, scalp tissues often interfere with the gray matter, white matter and CSF, which leads to inferior segmentation efficiency. Since the region of interest is the tumor portion, only the result of tumor segment is shown for the other two cases. Fig. 5 and Fig. 6 shows the qualitative analysis of the comparison of tumor segment with the phantom images for the moderate and mild cases.

In the above figures, a careful analysis of the input images is required to distinguish between the three stages of tumor which otherwise looks similar. Fig. 5 illustrates the ability of the proposed network for detecting the tumor even if the volume is low in the input image. In the case of mild stage image (Fig. 6), the tumor portion is hardly visible in the phantom image, which makes the segmentation process extremely difficult for the artificial neural network. But still a comparable accuracy is obtained for the HSBPN network. A quantitative comparison in terms of the performance measures is performed between the conventional BPN technique and the HSBPN to show the superior nature of the proposed network. Tab. III shows the segmentation efficiency results for both techniques.

From the above table, it is evident that the segmentation efficiency of the HSBPN is significantly higher than BPN. The average segmentation efficiency of

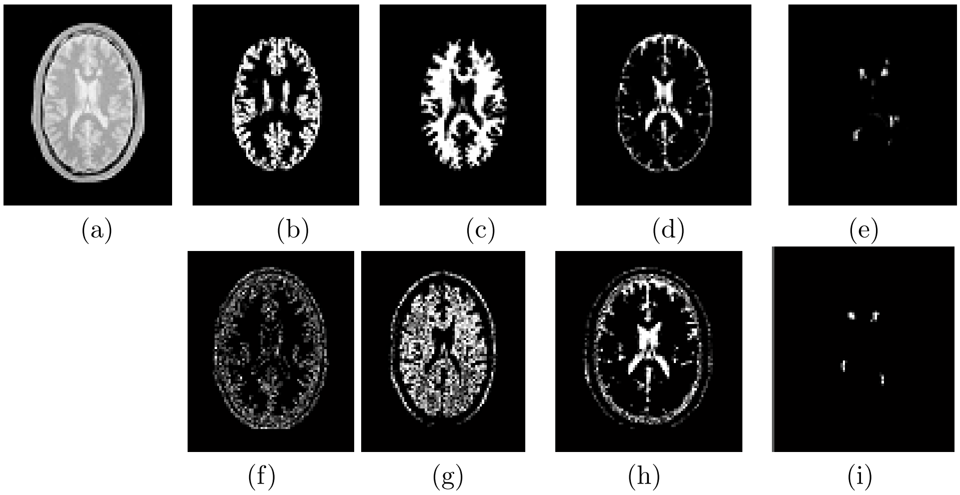

Fig. 4 *Severe image results: (a) Input image (b) Gray matter phantom (c) White matter phantom (d) CSF phantom (e) Tumor phantom (f) Gray matter segment (g) White matter segment (h) CSF segment (i) Tumor segment.*

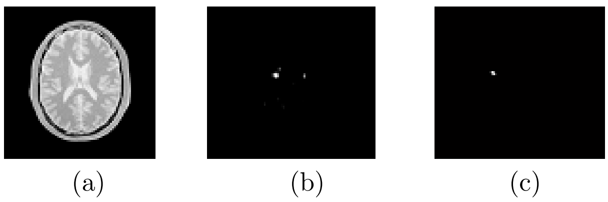

Fig. 5 *Moderate image results: (a) Input image (b) Tumor phantom (c) Tumor segment.*

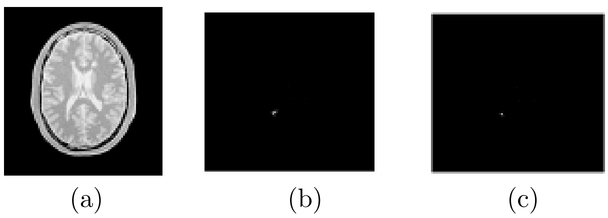

Fig. 6 *Mild image results: (a) Input image (b) Tumor phantom (c) Tumor segment.*

BPN is 74.85% and HSBPN is 85.2%. Thus, the proposed network successfully segments the tumor region even if it is small. Thus, the network is suitable for tumors of varying size and shape. Another analysis in terms of "false warnings" and

Input	No. of ground truth pixels	BPN		HSBPN	
		No. of correctly classified pixels	Segmentation efficiency (%)	No. of correctly classified pixels	Segmentation efficiency (%)
Severe stage	297	277	93	288	96
Moderate stage	86	72	83	75	87
Mild stage	21	10	47	15	71

Tab. III *Segmentation efficiency of BPN and HSBPN.*

"missed tumors" is also performed in this work. "False warnings" are the healthy pixels classified as abnormal pixels, and "missed tumors" are the abnormal pixels classified as normal pixels. A detailed analysis is given in Tab. IV.

Input	No. of Tumor pixels	BPN		HSBPN	
		False warnings (No. of pixels)	Missed tumors (No. of pixels)	False warnings (No. of pixels)	Missed Tumors (No. of pixels)
Severe stage	297	38	20	18	11
Moderate stage	86	52	14	24	11
Mild stage	21	71	11	29	6

Tab. IV *False warnings and missed tumor analysis.*

It is evident from the above table that the number of "false warnings" and "missed tumors" is very much smaller for the HSBPN. "Missed tumors", which are highly worse in medical diagnosis, are reduced to greater extent, which is an added advantage of the proposed network. The improvement in the accuracy is mainly due to the fact that target vectors are supplied to both the hidden and output layers directly. This concept has made the hidden layer supervised, whereas in BPN the hidden layer depends indirectly on the error value generated from the output layer neurons. Since supervised layers yield more accurate output, the efficiency of the HSBPN is significantly higher than the BPN.

The HSBPN is also superior in terms of convergence rate, which is evident from Tab. V.

The convergence time period includes the training time and testing time. From Tab. V, it is evident that the convergence rate of HSBPN is significantly higher than the conventional BPN technique. The convergence time period is highly reduced since the proposed technique is an iteration-free technique. This quantitative analysis clearly indicates that the HSBPN yields a superior convergence rate than the conventional BPN besides yielding comparable segmentation efficiency.

Techniques	Average training time period (CPU secs)	Average testing time period (CPU secs)
BPN	1658.9	0.365
HSBPN	9.7	0.3

Tab. V *Convergence time period of BPN and HSBPN.*

A comparative analysis among other neural networks in terms of the performance measures is shown in Tab. VI.

Neural Networks	Average Segmentation efficiency (%)	Average Convergence Time Period (CPU secs)
Radial Basis Function Networks	79	1580
Kohonen Networks	64	990
BPN	81	1660
HSBPN	87	10

Tab. VI *Performance measures of various artificial neural networks.*

Tab. VI clearly illustrates the advantages of the proposed method over the other artificial neural networks. Thus, this work suggests the HSBPN as a suitable replacement for conventional BPN.

8. Conclusion and Future Work

The convergence rate of the HSBPN is approximately 171 times superior to the conventional BPN. The proposed technique also eliminates the drawback of conventional BPN, which is iteration dependent for high segmentation efficiency. But the complexity of the proposed technique increases with the increase in the number of input features and the output classes. This problem can be solved by applying suitable optimization algorithms for feature selection. The proposed technique works well for tumor tissues of different size and shapes. As a future work, the segmentation efficiency of HSBPN may be improved by performing suitable modifications in the architecture and the algorithm. Emphasis may be also placed on feature extraction to improve the efficiency. Thus, this work proposes a neural network which segments the image much faster than the conventional network, which is highly essential for the medical field.

As an extension of this work, different feature sets can be used to train the network, which may improve the accuracy. Emphasis also may be given to feature selection using optimization techniques

References

[1] Kaus M. et al.: Automated segmentation of MRI brain tumors. Journal of Radiology, 218, 2001, pp. 585-591.

[2] Warfield S. K., Kaus M., Kikinis R.: Adaptive template moderated spatially varying statistical classification. Journal of Medical Image Analysis, 4, 2000, pp. 43-55.

[3] Dou W.: A framework of fuzzy information fusion for the segmentation of brain tumor tissues on MR images. Journal of Image and Vision Computing, 25, 2007, pp. 164-171.

[4] Pitiot A., Toga A. W., Thompson P. M.: Adaptive elastic segmentation of brain MRI via shape-model-guided evolutionary programming. IEEE Transactions on Medical Imaging, 21, 2002, pp. 910-923.

[5] Styner M., Szekley G., Gerig G.: Parametric estimate of intensity inhomogeneties applied to MRI. IEEE Transactions on Medical Imaging, 1, 2000, pp. 153-165.

[6] Leemput K. V., Maes F., Suetens P.: A unifying framework for partial volume segmentation of brain MR images. IEEE Transactions on Medical Imaging, 22, 2003, pp. 105-119.

[7] Ruan S., Moretti B., Bloyet D.: Fuzzy Markovian segmentation in application of MR images. Journal of Computer Vision and Image Understanding, 85, 2002, pp. 54-69.

[8] Ho S., Bullit S., Gerig G.: Level set evaluation with region competition:automatic 3-D segmentation of brain tumors. Proceedings of the International Conference on Pattern Recognition, 1, 2002, pp. 532-535.

[9] Udupa et al.: Multiple scelrosis lesion quantification using fuzzy connectedness principles. IEEE Transactions on Medical Imaging, 16, 1997, pp. 598-609.

[10] Saba K., Jayarama K.: Fuzzy connected object delineation:axiomatic path strength definition and the case of multiple seeds. Journal of Computer Vision and Image Understanding, 83, 2001, pp. 275-295.

[11] Zumray D., Tamer O., Ertugrul Y.: Biomedical image classification by using artificial neural networks. IEEE Proceedings of the 8th Mediterranean Electrotechnical Conference, Italy, 3, 1996, pp. 1469-1471.

[12] Li Y., Chi Z.: MR Brain Image Segmentation Based on Self-Organizing Map Network. International Journal of Information Technology, 11, 2005, pp. 45-57.

[13] Parra C., Khan I., Kozna R.: Automated brain data segmentation and pattern recognition using ANN. Proceedings of the International Conference on Computational Intelligence, Robotics and Autonomous Systems, 2003.

[14] Rezai-Rad G., Ebrahimi R. V.: Modified Fuzzy Hopfield Neural Network for MRI Image segmentation. Proceedings of the International conference on Biomedical and Pharmaceutical Engineering, 2006, pp. 58-61.

[15] Fausett L.: Fundamentals of Neural Networks: Architectures, Algorithms and Applications. Prentice Hall, New Jersey, 2002.

[16] Knowles A., Gibbs P., Turnbull L. W.: Improved classification of breast DCE-MRI using a neural network ensemble. In: Proc. Int. Soc. Magn. Reson. Med., 8, 2000, p. 2163.

[17] Changua Y. et al.: An efficient hidden layer training method for the multilayer perceptron. Journal of Neurocomputing, 70, 2006, pp. 525-535.

[18] Shamsudin S. M., Darus M., Sulaiman M. N.: Classification of reduction invariants with improved BPN. International journal of mathematics and mathematical sciences, 30, 2002, pp. 239-247.

[19] McConnell Brain Imaging Centre(McBIC), Montreal Neurological Institute, McGill University, `http://www.bic.mni.mcgill.ca/brainweb`.

[20] Haarlick R. M.: Statistical and structural approaches to texture. IEEE Transactions on System, Man and Cybernetics, 67, 1979, pp. 786-804.

[21] Gonzalez R., Woods R. E.: Digital Image Processing. Pearson Education, 2002.

[22] Xuan Xiao, Liao and Qingmin: Statistical structure analysis in MRI brain tumor segmentation. Proceedings of the International Conference on Image and Graphics, 22, 2007, pp. 421-426.

[23] Freeman J. A., Skapura D. M.: Neural Networks, Algorithms, Applications and Programming Techniques. Addison – Wesley, 2002.

[24] MATLAB User's Guide, The Math Works, Inc., Natick, MA 01760, 2002.